Exchange of Monooleoylphosphatidylcholine with Single Egg Phosphatidylcholine Vesicle Membranes

Doncho V. Zhelev
Department of Mechanical Engineering and Materials Science, Duke University, Durham, North Carolina 27708-0300 USA

ABSTRACT In a previous paper we described the experiments and the framework of a model for the exchange of monooleoylphosphatidylcholine with a single egg phosphatidylcholine membrane. In the present paper a model is presented that relates the experimentally measured apparent characteristics of the overall kinetics of lysolipid exchange to the true rates of lysolipid exchange and interbilayer transfer. It is shown that the adsorption of the lysolipid follows two pathways: one through the adsorption of lipid monomers and other through the fusion of micelles. The desorption of lysolipid follows a single pathway, namely, the desorption of monomers. The overall rate of fast desorption under convective flow conditions gives the true rate of monomer desorption from the outer membrane monolayer. The overall rate of both slow lysolipid uptake and slow desorption gives the rate of interbilayer transfer. Because of the uneven distribution of lysolipid between the two monolayers during its uptake, one of the membrane monolayers is apparently extended relative to the other. This relative extension of one of the monolayers induces a monolayer tension. The induced monolayer tension can increase up to 7 $mN \cdot m^{-1}$, when most of the intercalated lysolipid only partitions into the monolayer facing the lysolipid solution. This value is similar to the measured value for the critical monolayer tension of membrane failure, which is on the order of 5 $mN \cdot m^{-1}$. The similarity of the magnitudes of the induced monolayer tension during monooleoylphosphatidylcholine exchange and the monolayer tension of membrane failure suggests that the interbilayer lipid transfer may be affected by the formation of short living membrane defects. Furthermore, the pH-induced interbilayer exchange of phosphatidylglycerol is considered. In this case, it is shown that the rate of interbilayer transfer is a function of the phosphatidylglycerol concentration in the membrane.

GLOSSARY

a_o^b	area per molecule at zero membrane tension for the lipid forming the bilayer membrane
a_o^l	area per molecule at zero membrane tension of the exchangeable lipid
A_m	area of the vesicle membrane
$\alpha^{e,b}$ and $\alpha^{e,l}$	fractional area changes of the diacyl lipid and the lysolipid, respectively (the fractional area change is equal to the ratio of the area change to the initial area)
C_b	bulk concentration of lysolipid in the bathing solution
E_b	barrier energy
ΔG	energy of dissociation
$\Delta G^{\ddagger}$	Gibbs energy of activation in standard state
$\Delta H^{\ddagger}$	enthalpy of formation of the activated state
$\hbar$	Planck's constant
J_{mb} and J_{bm}	molecular fluxes toward the membrane and toward the bathing solution, respectively
k	Boltzmann constant
K^b	area expansion modulus of a diacyl lipid
K^l	area expansion modulus of a lysolipid
k_{mb}	rate of lysolipid monomer dissociation or "off" rate
k'_{bm}	rate of lysolipid monomer association or "on" rate
k'_{bm}	rate of micelle fusion
k_f	rate of interbilayer transfer
N_A	Avogadro's constant
N^l_{mi} or N^l_{mo}	number of lysolipid molecules in the inside and outside membrane monolayers
N^b_m	number of diacyl lipid molecules in the membrane
p'	mass transport coefficients of the stagnant layer for lysolipid monomers
p''	mass transport coefficients of the stagnant layer for micelles
R	gas constant
τ_α	applied membrane tension
τ_i and τ_o	monolayer tensions of the inside and outside membrane monolayers, respectively
$\Delta S^{\ddagger}$	entropy of formation of the activated state
T	absolute temperature
Z^* and Z_m	partition functions of the activated state and the metastable state

Received for publication 20 July 1995 and in final form 15 April 1996.

Address reprint requests to Dr. Doncho V. Zhelev, Department of Mechanical Engineering and Materials Science, Duke University, Durham, NC 27708-0300. Tel.: 919-660-5372; Fax: 919-660-8963; E-mail: dvzh@acpub.duke.edu.

0006-3495/96/07/257/17 $2.00

INTRODUCTION

Lysophosphatidylcholine (LPC or lysolipid) is an important molecule for a range of cellular processes that involve

signaling, receptor-mediated adhesion, and membrane breakdown. It is produced after hydrolysis of phospholipids catalyzed by phospholipase A_2 (Brown et al., 1993; Baker et al., 1994) or the oxidation of low-density lipoprotein (LDL) (Quinn et al. 1988; Mangin et al., 1993). It plays a role in many cell functions, including the regulation of guanylate and adenylate cyclase activities (Shier et al., 1976) and chemotaxis of human monocytes (Quinn et al., 1988; Nakano et al., 1994) and mouse thymus lymphoma cells (Hoffman, 1982). The incubation of endothelial cells with LPC leads to an increase in the expression of adhesion molecules for monocytes, such as the vascular cell adhesion molecule (VCAM-1) and the intercellular adhesion molecule (ICAM-1) (Kume et al., 1992). The inhibition of LPC acylation enhances the production of platelet activation factor by polymorphonuclear leukocytes (Naraba et al., 1993) and affects the relaxation of the vascular smooth muscle (Saito et al., 1988). The activation of T-lymphocytes by phospholipase A_2 involves lysophosphatidylcholine (Asaoka et al., 1993). When LPC partitions into membranes at relatively high concentrations, it arrests membrane fusion (Vogel et al., 1993), and at even higher concentrations it substantially decreases the strength of the membrane and leads to membrane lyses (Golan et al., 1986; Zhelev, submitted for publication). Important to all these processes is the partitioning of LPC into and out of the membrane. In this work, the passive transport and the partitioning of LPC in the membrane is modeled by using the kinetic approach.

The processes that involve LPC are likely to depend to a large part on the kinetics of its exchange with the membrane. Besterman and Domanico (1992) have shown that the partitioning of LPC in the membrane of mammalian cells is concentration dependent and is reversible. This observation suggests that the exchange of LPC with the cell membrane is passive and can be studied by using model membranes, which provide well-defined experimental conditions. Compared with the diacyl lipids that make up the bulk of the bilayer membrane, LPC has a much higher solubility in water (its critical micelle concentration is 10^{-7} to 10^{-4} M, depending on its chain length, which is much higher than the critical aggregation concentration of 10^{-10} M or less for the bilayer lipids; Marsh, 1990). As a result of this high solubility in both the membrane and aqueous solutions, LPC has a fast rate of exchange (on the order of 0.2 s^{-1}; Needham and Zhelev, 1995) between the two phases. Because of this fast rate of exchange, LPC transport cannot be studied by many of the commonly used methods, such as radiolabeling, which requires a longer time before starting the measurements than the half-time of the lysolipid exchange. The intercalation of the lysolipid in the membrane also affects the membrane's tensile strength (Zhelev, submitted for publication), which may also alter membrane permeability. This makes it difficult to use other methods, such as fluorescence labeling, when they are not coupled to measurements of membrane permeability.

The exchange of lysolipids with cell membranes has been studied by observing the shape change of closed membranes, such as the red blood cell membrane (Daleke and Huestis, 1985; Ferrell et al., 1985a,b). Initially, the lysolipid is believed to intercalate in the outer membrane monolayer. This initial intercalation leads to an apparent expansion of this monolayer. The expansion of the outer monolayer generates a bending moment, which leads to a crenation of the red cell membrane (Ferrell et al., 1985a). This effect is also observed in vesicle membranes (Farge and Devaux, 1992). Monitoring the shape change of these membrane capsules allows the main stages of lysolipid exchange to be determined, namely, lysolipid intercalation in the outer membrane monolayer and its transfer to the inner monolayer. Of those two stages, monolayer intercalation is usually much faster than interlayer transfer. However, observations of shape change have a very limited ability to provide quantitative kinetic data. Quantitative data are best provided by using methods that measure parameters related to the number of exchanged molecules, such as the change of membrane area (Elamrani and Blume, 1982; Needham and Zhelev, 1995). In the method developed by Needham and Zhelev (1995), lysolipid exchange is quantified by measuring the change of the projected area of a giant (20- to 40-μm diameter) vesicle membrane in a micropipette (Needham and Zhelev, 1995). The method is used to study the exchange of monooleoylphosphatidylcholine (MOPC) with a single vesicle membrane made of egg phosphatidylcholine (EPC). The exchanged lysolipid and the diacyl phospholipid making up the membrane have the same headgroups, and their hydrocarbon chains are of a similar length. The major difference between the two lipids is their number of hydrocarbon chains (MOPC has one hydrocarbon chain and EPC has two). In this work a model is presented in which the measured parameters of the overall kinetics of MOPC exchange are related to the true rates of lysolipid association ("on" rate), dissociation ("off" rate), and interbilayer transfer. The model also takes into account micelle-membrane fusion, when the concentration of MOPC in the bathing solution is above its critical micelle concentration (CMC). This model can be used only for analyzing data from flow experiments (Needham and Zhelev, 1995), where the concentration of MOPC in the bathing solution is constant.

MODEL OF LYSOLIPID EXCHANGE

The model of passive MOPC exchange is illustrated in Fig. 1. The exchange is between the membrane of a single vesicle and its bathing solution. Upon exposure of the vesicle to a solution of MOPC, the lysolipid starts to adsorb and intercalate in the outer membrane monolayer. This adsorption involves MOPC monomers, which follow the generally accepted scheme of exchange of diacyl lipids (Storch and Kleinfeld, 1986), and above the CMC it also involves MOPC micelles. The intercalated lipid is eventually transferred into the inner monolayer and desorbs into the vesicle interior. In this approach, the exchange with the vesicle interior is neglected because the amount of desorbed

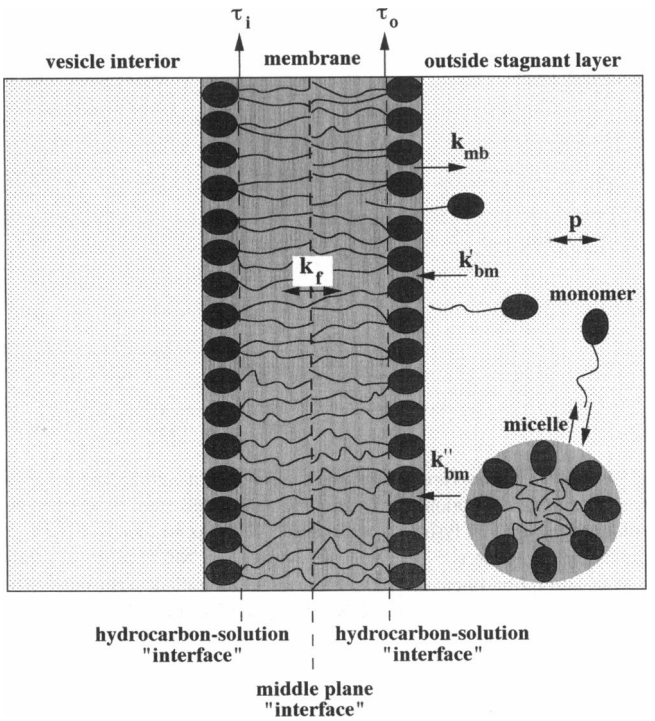

FIGURE 1 Schematic diagram of the exchange of MOPC with EPC vesicles. MOPC is transported from the bathing solution into the outer membrane monolayer as both monomer (characterized by the rate of intercalation or the "on" rate k'_{bm}) and micelle (characterized by the rate of micelle-membrane fusion k''_{bm}). The intercalated lysolipid is desorbed back into the bathing solution (characterized by the rate of dissociation or the "off" rate k_{mb}) or is transferred into the inner membrane monolayer (characterized by the rate of transfer k_f). The exchange with the vesicle interior is not included in the model, because the amount of MOPC in this aqueous region is negligible compared to its amount in the membrane (Needham and Zhelev, 1995). The transport of MOPC in the bathing solution depends on the mass transport coefficient of the stagnant layer p. During the exchange, the vesicle membrane is subjected to a tension. Because of the uneven distribution of the lysolipid between the two membrane monolayers, the tensions of the inner monolayer τ_i and that of the outer monolayer τ_o may be different.

lysolipid is negligible compared to its amount in the membrane (Needham and Zhelev, 1995).

In the experiments of Needham and Zhelev (1995), a single vesicle is also transferred from a solution with MOPC into a solution that is free of MOPC. In this case, lysolipid monomers from the outer monolayer are desorbed into the bathing solution, and this desorption is coupled with lipid transfer from the inner monolayer.

The exchange of lysolipid in the above processes is modeled as a molecular transport between three volumes: the two membrane monolayers and the outside bathing solution. The volumes are separated by apparent "interfaces." The amount of molecules transported across a given "interface" is characterized by the net flux across it. The molecular transport from the bathing solution into the membrane has two components: one is the transport of monomers from bulk solution to the membrane, characterized by the "on" rate k'_{bm}, and the other is the transport of micelles from bulk solution to the membrane, characterized by the rate of micelle fusion k''_{bm} (the subscript m refers to the membrane and subscript b to the bulk solution, respectively, and single prime refers to monomer and double prime to micelles, respectively). The molecular transport from the membrane into the bathing solution has one component, namely monomer dissociation, which is characterized by the "off" rate k_{mb}. Interbilayer transport proceeds with a rate called the rate of interbilayer transfer, k_f. Of the above processes, only monomer dissociation has been described in the literature so far. The model of monomer dissociation, proposed by Aniansson et al. (1976), considers a diffusion-limited transport for monomer dissociation that is limited to distances scaled by the length of the transported molecule.

In addition to the molecular exchange at the "interfaces" of the lipid pools in Fig. 1, MOPC is also transported within the volume of the bathing solution. This transport has diffusion and convection components. In the presence of flow, the convection component dominates when far from the membrane "interface," whereas transport of MOPC near the "interface" is always diffusion limited (Fettiplace and Haydon, 1980). The region closest to the membrane interface, where the transport is always diffusion limited, is called the unstirred or stagnant layer. For a spherical surface, such as the vesicle membrane, the molecular flux across the stagnant layer is proportional to the difference between the concentration of MOPC at the membrane "interface" and its concentration in the bathing solution. This flux is characterized by the stagnant layer's mass transport coefficient p (Friedlander, 1957).

As has already been pointed out, the apparent rate of exchange of MOPC with the bathing solution is much faster than the rate of its interbilayer transfer. This difference in the two rates leads to a difference in the lysolipid partitioning in the two monolayers. The monolayer with lower partitioning of MOPC becomes extended relative to the one with higher partitioning of the lysolipid. The area per molecule in the extended monolayer is therefore slightly larger than the area per molecule in the membrane of its standard state. (The standard state of the membrane is its state in the absence of MOPC. In this case, the area per molecule is set by the applied membrane tension or the corresponding pipette suction pressure.) The increase in the area per molecule resulting from the unequal distribution of lysolipid between membrane monolayers may reach values similar to the ones measured for membrane breakdown that results from applying large membrane tensions. Then the extended monolayer is expected to "fail" and to form short-lived "monolayer defects." These "defects" will have a lower barrier energy for lipid transfer compared to the "standard" bilayer membrane and are expected to affect the rate of interbilayer lipid transfer.

The experimentally measured kinetics of MOPC exchange is a double exponential with fast and slow components (Needham and Zhelev, 1995). The measured rate of the fast component is 0.2 s^{-1} and that of the slow component is 0.002 s^{-1}. Other experimental observations are 1)

Above the CMC, the apparent rate of fast adsorption is usually slower than the rate of fast desorption, and both rates depend on the mode of transport in the bathing solution (convective transport provides faster overall rates of exchange than diffusion). 2) The amount of MOPC intercalated into the membrane depends on the lysolipid concentration in the bathing solution both below and above the CMC, i.e., both monomer and micelles are active species in promoting lysolipid uptake into the membrane. 3) When, during fast adsorption, the relative area increase reaches the limit of 6–8%, the volume of the vesicle starts to change, i.e., a critical lysolipid concentration in the membrane leads to the formation of membrane defects (pores) that allow the vesicle volume to change by the transport of osmolarity active solutes.

The observed difference between the apparent rate of fast uptake and fast desorption could be explained if MOPC is transported into the membrane both as a monomer and a micelle, while it desorbs as a monomer. This difference can also be explained if the rates of exchange depend on the concentration of lysolipid in the membrane. The exchange of MOPC in the first case is called "exchange with constant rates," and that in the second case "exchange with functional rates."

DEPENDENCE OF THE MEASURED BILAYER VESICLE AREA CHANGE ON THE NUMBER OF INTERCALATED MOLECULES

During the exchange of MOPC between the bathing solution and the vesicle membrane, the total number of MOPC molecules in the membrane changes (during MOPC adsorption this number increases and during desorption it decreases). The change in the number of molecules in the membrane is monitored by measuring the change in its area (Needham and Zhelev, 1995). Fig. 2 illustrates the measured area change of a vesicle membrane during the fast adsorption of MOPC and its fast desorption, in one of the experiments of Needham and Zhelev (1995). During the fast exchange, MOPC partitions mainly in the outer monolayer of the vesicle bilayer. The area increase in this case is exponential and eventually slows down as the outer monolayer is saturated with MOPC. The fast desorption is also exponential (but faster), and the final area of the vesicle is similar to its initial area, suggesting that MOPC is almost completely desorbed from the membrane.

During the course of MOPC exchange, the number of lysolipid molecules in the two membrane monolayers may be significantly different. For example, during MOPC adsorption this difference is maximum at the end of the fast kinetics, when the outer monolayer is almost saturated with MOPC and the amount of lysolipid in the inner monolayer is still negligible. The two monolayers of the giant vesicle membranes used in the experiments of Needham and Zhelev (1995) have equal areas. Thus, the addition of MOPC to the outside monolayer leads to an actual expansion of the inside

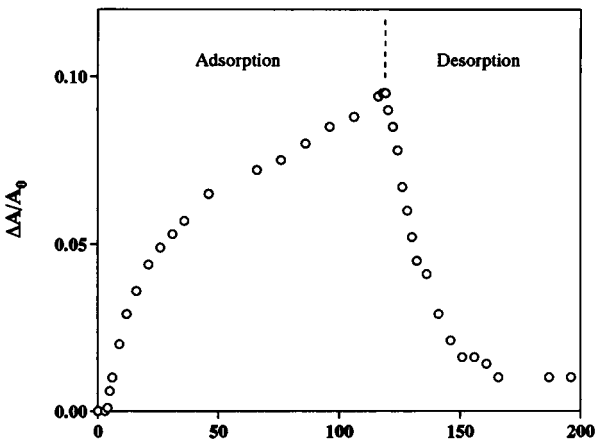

FIGURE 2 Relative area change ($\Delta A/A_0$) of the membrane for a single vesicle during adsorption-intercalation of a lysolipid from 5 μM MOPC solution followed by lysolipid desorption. The concentration of MOPC in the bathing solution is 5 μM, which is above the CMC, and the apparent rate of adsorption-intercalation is slower than the rate of desorption. The data are from the experiments of Needham and Zhelev (1995).

monolayer. This expansion occurs at an almost constant number of molecules of this monolayer and, therefore, is coupled with an increase in the monolayer tension. While the tension of the inside monolayer increases, the total tension of the bilayer membrane remains constant. (This latter tension is equal to the applied tension, which is set by the suction pipette.) The constraint of constant total membrane tension requires that the tension of the outside monolayer decreases (and to even become negative or to convert to "tension of compression"), while the tension of the inside monolayer increases. This scenario of coupling the area changes and the induced tensions of the two membrane monolayers is used to calculate the number of MOPC molecules partitioning in the membrane from the measured relative area change ($\Delta A/A$),

$$\frac{\Delta A}{A} = \frac{a_o^l}{2A}\left(1 + \frac{\tau_\alpha}{2K^l}\right) \cdot (N_{mi}^l + N_{mo}^l) - O(a_o^b, a_o^l, K^b, K^l, N_{mi}^b, N_{mo}^b, N_{mi}^l, N_{mo}^l, \tau_\alpha, A), \quad (1)$$

where a_o^b and a_o^l are the areas per lipid molecule at zero membrane tension of EPC and MOPC, respectively; K^b and K^l are their respective area expansion moduli; N_{mi}^b and N_{mo}^b, and N_{mi}^l and N_{mo}^l are the numbers of molecules in the inside and outside monolayer for EPC and for MOPC, respectively; A is the initial area of the vesicle; τ_α is the applied membrane tension set by the pipette; and the functional factor $O(a_o^b, a_o^l, K^b, K^l, N_{mi}^b, N_{mo}^b, N_{mi}^l, N_{mo}^l, \tau_\alpha, A)$ is defined in Appendix I.

It is seen that the change in the membrane area is proportional to the intercalated lipid plus a factor called a distribution factor. The distribution factor is zero for equally distributed lysolipid and is at a maximum when all of the intercalated MOPC remains in one of the membrane monolayers.

The dependence of the measured area change on the lysolipid distribution between the two membrane monolayers can be found when the area per molecule and the area expansion modulus of the lipids making up the membrane are known. The area per molecule and the area expansion modulus of EPC are 65 Å^2 (McIntosh and Simon, 1986) and 167 mN·m^{-1} (McIntosh et al., 1994), and that of MOPC are 35 Å^2 and 150 mN · m^{-1}. [The area per MOPC molecule in EPC membrane is calculated using the x-ray data of pure EPC and (1:1) EPC:MOPC membranes (McIntosh et al., 1995). The thickness of (1:1) EPC:MOPC membrane is 1 Å less than that of EPC membrane. Furthermore, the shapes of the electron density profiles at the region of the phosphate group in the two cases are identical. These results, taken together, suggest that the addition of MOPC to EPC membrane does not significantly affect its structure, and that the headgroups of MOPC and EPC are in the same plane (McIntosh et al., 1995). Using these observations and the assumption that the hydrophobic region of the membrane is incompressible, the area of MOPC in EPC membrane is calculated to be 35 Å^2. The area expansion modulus of MOPC is calculated from the measured area expansion modulae of EPC membranes containing different amounts of MOPC (Zhelev, submitted for publication).] The theoretical dependence of the area increase on the distribution of MOPC for a membrane with 5, 20, and 40 mol% lysolipid is shown in Fig. 3. It is seen that the deviation of the relative area increase from its value for equally distributed MOPC does not exceed 10%, even when all of the MOPC is in one of the monolayers.

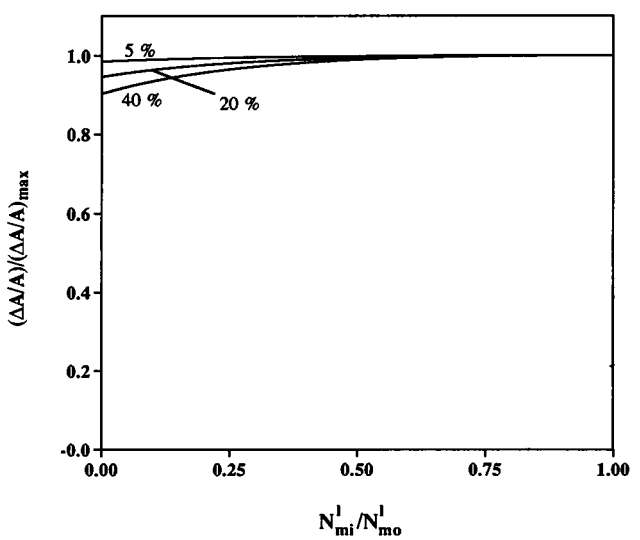

FIGURE 3 Normalized relative area increase $((\Delta A/A_0)/(\Delta A/A_0)_{max})$ as a function of the ratio of the relative number of MOPC molecules N^l_m in the inner (i) and the outer (o) membrane monolayers. The relative area increase is normalized by the relative area increase for the case of equally distributed MOPC. The relative area increase is calculated for MOPC concentrations of 5 mol%, 20 mol%, and 40 mol%. The applied membrane tension is 1 mN · m^{-1}, which is the tension used in the experiments of Needham and Zhelev (1995).

In the experiments of Needham and Zhelev (1995), fast saturation of the outside monolayer is achieved by using the flow of MOPC solution over the test vesicle. In this case, the exchange of MOPC follows the model in Fig. 1 until the relative area increase of the vesicle membrane reaches 6–8%, when pores start to form. A relative area increase of 6–8% corresponds to 10 to 15 mol% MOPC in the membrane. This molar concentration of MOPC sets the limit for using the presented model for the case of fast saturation. In contrast to the fast saturation regime, the slow saturation regime (when the flow of MOPC-containing solution is a few microns per second) allows total lysolipid uptake to increase to 35 mol% or more (Needham and Zhelev, 1995). These results show that, depending on the experimental conditions, the maximum MOPC uptake by a stable bilayer may be from 10 to 40 mol%. Fig. 3 shows the dependence of the relative area increase on the lysolipid distribution for 5, 20, and 40 mol% MOPC. From this figure it is seen that for fast saturation, when MOPC uptake is 15 mol% or less, the error due to the unknown distribution does not exceed 10%. For slow saturation, when MOPC uptake is up to 40 mol%, the difference in MOPC distribution is small and the error again is less than 10%. This result shows that for MOPC the distribution factor is small compared to the first term of Eq. 1.

Fig. 4 presents the dependence of the area increase on the molar concentration of MOPC, when all of the lysolipid is in one of the monolayers calculated according to Eq. 1. It is seen that this dependence is almost linear. The results from Figs. 3 and 4 show that the molar concentration of MOPC calculated from the first term of Eq. 1 gives a reliable estimate of its true membrane concentration.

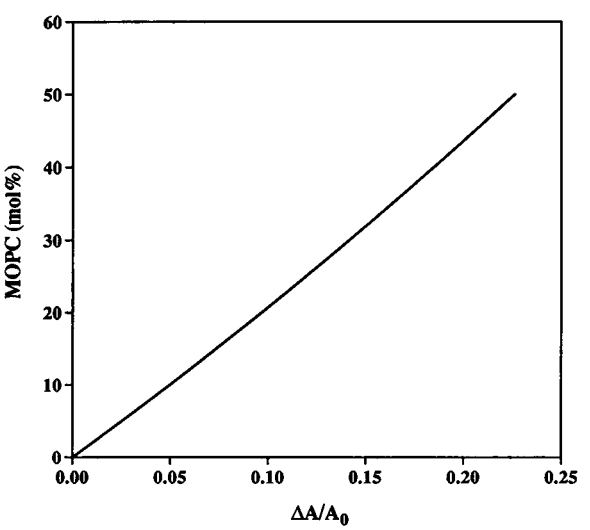

FIGURE 4 Molar concentration of MOPC in the membrane versus the relative area increase at the end of the fast MOPC exchange. In this case, the lysolipid concentration in the inner monolayer is negligible compared to its concentration in the outer monolayer. The applied membrane tension is 1 mN · m^{-1}.

EXCHANGE WITH CONSTANT RATES

(Exchange with constant rates is the exchange, where the "on" rate, the "off" rate, and the rate of interbilayer transfer are independent of the amount of transported LPC.)

Single monolayer

During the fast exchange of MOPC, the lysolipid remains mainly in the outer monolayer. In this case, the exchange occurs between the outer monolayer and the outside bathing solution. The experiments of Needham and Zhelev (1995) show that in this case, the overall rate dN_{mo}/dt of exchange is strongly dependent on the stagnant layer. Furthermore, the rate of intercalation is different for MOPC concentrations in the bathing solution that are either above or below the CMC. The rate of desorption is independent of the amount of intercalated MOPC. Above the CMC, the apparent rate of adsorption is slower than the apparent rate of desorption (see also Fig. 2).

The kinetics of MOPC intercalation and desorption below the CMC is given by (see Appendix II)

$$N_{mo} = f_1(k_{mb}, k'_{bm}, A_m, C_{b\infty}) + f_2(k_{mb}, k'_{bm}, A_m, C_{b\infty}, N_{imo})\exp\left(-\left(\frac{k_{mb}}{1+\frac{A_m k'_{bm}}{p'}}\right)t\right), \quad (2)$$

where N_{mo} is the number of MOPC molecules in the membrane, k_{mb} is the "off" rate, k'_{bm} is the "on" rate, p' is the mass transport coefficients for MOPC monomers, A_m is the membrane area, f_1 and f_2 are coefficients (for the definition of the functional coefficients see Eq. AII.4) and the quantity $k_{mb}/(1 + A_m k'_{bm}/p')$ is the experimentally measured apparent rate of exchange.

The kinetics of MOPC adsorption above the CMC is given by

$$N_{mo} = f_1(k_{mb}, k'_{bm}, k''_{bm}, A_m, \mathrm{CMC}, C''_{b\infty}) + f_2(k_{mb}, k'_{bm}, k''_{bm}, A_m, \mathrm{CMC}, C''_{b\infty}, N_{imo})\exp\left(-\left(\frac{k_{mb}}{1+\frac{A_m k''_{bm}}{p''}}\right)t\right), \quad (3)$$

where k''_{bm} is the rate of MOPC intercalation due to micelle-membrane fusion, p'' is the mass transfer coefficients for MOPC micelles, and the coefficients f_1 and f_2 are defined in Eq. AII.7.

The dependence of both the apparent rate of MOPC intercalation (Eqs. 2 and 3) and desorption (Eq. 2) on the mass transport coefficients is similar. Above the CMC the apparent rate of intercalation may be different from the apparent rate of desorption because the mass transport coefficient in Eq. 3 may be different from that in Eq. 2. This behavior is illustrated in Fig. 5, where curve 1 is for 0.5 μM MOPC (which is below the CMC), and curve 2 is for 5 μM MOPC (which is above the CMC). It is seen that below the CMC (curve 1) both the kinetics of intercalation and desorption have the same apparent rate, whereas above the CMC (curve 2) the apparent rate of intercalation is slower than the apparent rate of desorption. This result is in agreement with the experiment as shown in Fig. 2. The dependence of the apparent rate of intercalation and the apparent rate of desorption on the mass transport coefficient is shown in Fig. 6 (in this example the "off" rate is equal to 0.2 s^{-1}). Curve 1 shows the apparent rate of intercalation above the CMC, and curve 2 shows the apparent rate of desorption (which is also the apparent rate of intercalation below the

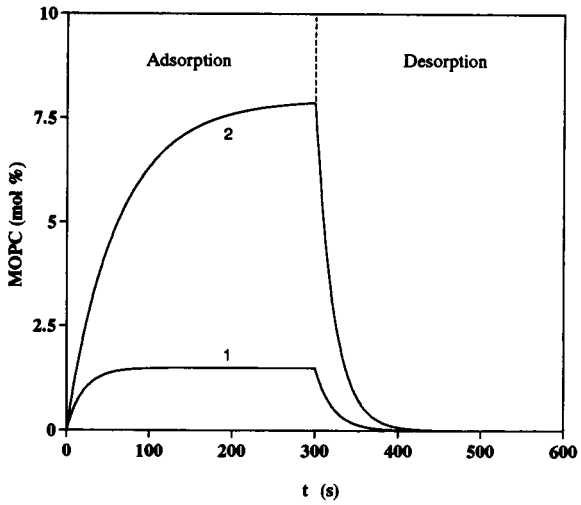

FIGURE 5 Molar concentration of MOPC in the outer membrane monolayer calculated from Eq. AII.4 (curve 1) and Eq. AII.7 (curve 2). The concentration of MOPC in the two examples is 0.5 μM (curve 1) and 5 μM (curve 2), respectively. The parameters used in the model are CMC = 0.7 μM; k_{mb} = 0.2 s^{-1}; k'_{bm} = 0.003 cm · s^{-1}; k''_{bm} = 0.0015 cm · s^{-1}; p' = 3 × 10^{-8} $cm^3 \cdot s^{-1}$; and p'' = 0.13 p'. The overall kinetics is a single exponential with one apparent rate of exchange.

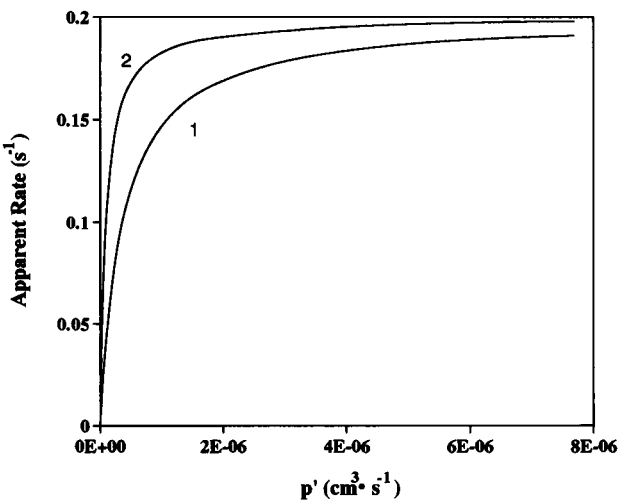

FIGURE 6 Dependence of the apparent rate of adsorption above the CMC (curve 1) and the apparent rate of desorption (which is also the apparent rate of adsorption below the CMC) (curve 2) on the mass transfer coefficient of the stagnant layer (the parameters are the same as in Fig. 5).

CMC). It is seen that for small mass transfer coefficients the magnitude of both apparent rates is much smaller than the "off" rate of 0.2 s^{-1}. In these cases, the experimentally measured kinetics is mostly dominated by the stagnant layer. For intermediate values of the mass transfer coefficients, the apparent rate of adsorption depends more strongly on the stagnant layer than on the rate of desorption, because the diffusion of MOPC micelles is slower than the diffusion of monomers. For large mass transfer coefficients, the two apparent rates are similar and are close to the true "off" rate. This result can be used to find experimental conditions in which the role of the stagnant layer is at a minimum, and to calculate the error in determining the "off" rate from the experimentally measured apparent rates. The mass transfer coefficient for monomers and for micelles is calculated by using its definition after Eq. AII.3. The diffusion coefficients of MOPC monomers and micelles are chosen to be equal to 5×10^{-10} $m^2 \cdot s^{-1}$ and 1×10^{-10} $m^2 \cdot s^{-1}$, respectively. The size of the vesicle is chosen to be 15 μm. For these conditions, the apparent rate of MOPC intercalation and the rate of desorption are close to the true "off" rate only when convective flow velocities that are used to deliver MOPC to the vesicle surface are on the order of a few thousands of $\mu m \cdot s^{-1}$. Velocities of this magnitude are sufficient to break a vesicle membrane that contains MOPC. For the flow rates used in the experiments of Needham and Zhelev (1995) (on the order of hundreds to thousands of $\mu m \cdot s^{-1}$), the measured apparent rates are about 20% smaller than the "off" rate. Equation 3 also predicts that the membrane partitioning of MOPC at steady-state conditions always depends on the micelle concentration in the bathing solution. Therefore, it is possible by increasing the concentration of lysolipid in the bathing solution to increase MOPC partitioning in the membrane at ratios that are sufficient to promote membrane breakdown or even to dissolve the membrane by the formation of a stable micellar phase.

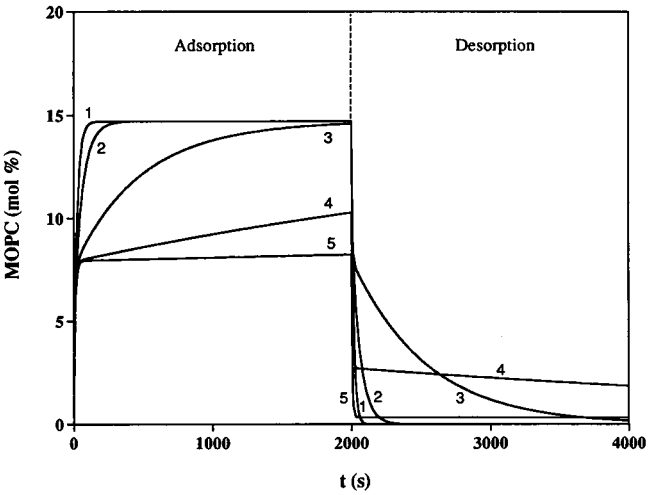

FIGURE 7 Molar concentration of MOPC calculated from Eq. AII.10. The parameters of the model are the same as in Fig. 5. Different curves correspond to different rates of interbilayer transfer: curve 1, $k_f = 1 \times 10^{-1}$ s^{-1}; curve 2, $k_f = 1 \times 10^{-2}$ s^{-1}; curve 3, $k_f = 1 \times 10^{-3}$ s^{-1}; curve 4, $k_f = 1 \times 10^{-4}$ s^{-1}; curve 5, $k_f = 1 \times 10^{-5}$ s^{-1}. For intermediate values of the rate of interbilayer transfer, the overall kinetics is a double exponential. The apparent rate of the fast exponential is determined by the rate of saturation of the outside monolayer, and the apparent rate of the slow exponential is determined by the rate of interbilayer transfer.

Bilayer membrane

For the whole bilayer, the kinetics of MOPC exchange for long time intervals is a double exponential, because it involves exchange with the outer monolayer and transfer of lysolipid between the two membrane monolayers,

$$N_m = \sum_{i=0}^{2} \prod_{\substack{j=0 \\ j \neq i}}^{2} \frac{\exp(s_i t)}{(s_i - s_j)} (s_i(s_i + 2k_f)N_{imo} + s_i\left(s_i + \frac{k_{mb}}{\beta} + 2k_f\right)N_{imi} + (s_i + 2k_f)\eta). \quad (4)$$

(The coefficients of Eq. 4 are defined in Appendix II.)

The kinetics given by Eq. 4 has both fast and slow components. The apparent rate of the fast component is determined by the "off" rate, and the apparent rate of the slow component is determined by the rate of interbilayer transfer. The dependence of the overall kinetics on the rate of interbilayer transfer is shown in Fig. 7. When the rate of interbilayer transfer is on the order of the "off" rate or faster, the overall kinetics is apparently a single exponential. When it is up to three orders of magnitude smaller than the "off" rate, the kinetics is a double exponential. This is the case for MOPC, where the "off" rate is on the order of 0.2 s^{-1} and the rate of interbilayer transfer on the order of 0.002 s^{-1} (Needham and Zhelev, 1995). When the rate of interbilayer transfer is much smaller than the "off" rate (e.g., for

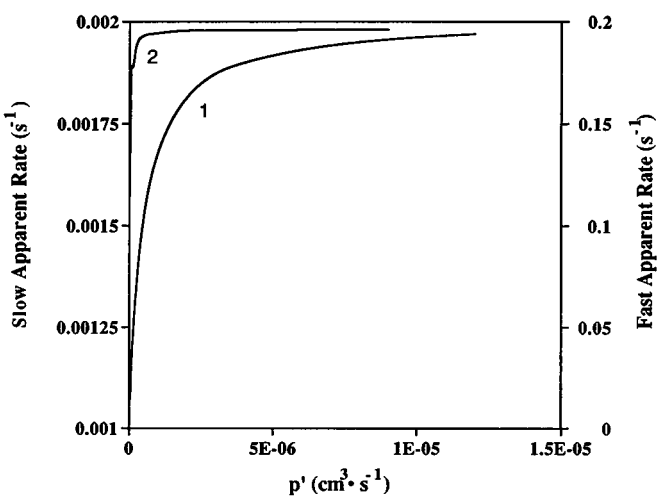

FIGURE 8 Dependence of the slow apparent rate (curve 2) and the fast apparent rate (curve 1) of MOPC exchange above CMC on the mass transfer coefficient of the stagnant layer.

well-packed membranes, such as membranes below the phase transition; Wimley and Thompson, 1990, 1991), the kinetics is single exponential and the amount of transferred lipid is negligible.

Fig. 8 shows the dependence of the fast component and the slow component of the overall kinetics on the stagnant layer. It is seen that the fast component (curve 1) has the same dependence on the stagnant layer as the overall kinetics of MOPC exchange with a single monolayer. The slow component does not depend on the stagnant layer, except at very small values of the mass transfer coefficient. For the experimental conditions in the experiment of Needham and Zhelev (1995) the slower component is not affected by the stagnant layer.

EXCHANGE WITH FUNCTIONAL RATES

(Exchange with functional rates is the exchange, where the "on" and the "off" rate as well as the rate of interbilayer exchange depend on the amount of transported molecules.)

Exchange with the outer monolayer

The uptake of MOPC in the membrane may reach 30 mol% or more (Needham and Zhelev, 1995; Van Echteld et al., 1981). This leads to a substantial change in the composition of the membrane. Wimley and Thompson (1990, 1991) have shown that lipid composition is one of the factors that can determine the rates of exchange. Therefore, the adsorption of MOPC itself is expected to affect the exchange rates. In this case, the "on" and the "off" rates as well as the rate of interbilayer transfer will be functions of the number of exchanged molecules. In this section, it is shown how the dependence of the above rates on the number of transported molecules may affect the fast lysolipid exchange with the outside monolayer. For simplicity the effect of the stagnant layer is neglected. (Indeed, in the previous sections it has been shown that for fast exchange the overall kinetics of MOPC uptake is governed mainly by the "on" and the "off" rate, whereas the stagnant layer accounts for 20% or less of the measured apparent rate.) It is assumed also that both the "on" and the "off" rates are analytical functions of the number of intercalated molecules and only the first two terms of their Taylor expansion are considered.

The kinetics of molecular exchange in this case is given by

$$N_{mo} = f_0 - f_1 \frac{\exp(-t\sqrt{b^2 + 4ac})}{(f_2 + \exp(-t\sqrt{b^2 + 4ac}))}. \quad (5)$$

(The definition of the coefficients in Eq. 5 is given in Appendix III.)

The initial kinetics is complex, but it eventually becomes a single exponential because the exponential in the denominator becomes much smaller than the absolute value of f_2. Fig. 9 shows the kinetics of intercalation for different values of k_{mb1}, k^{1}_{bm1}, and k''_{bm1}. The values of these coefficients are

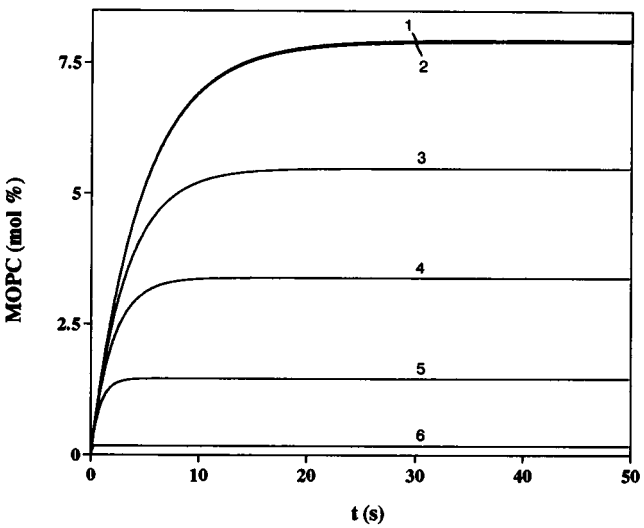

FIGURE 9 Molar concentration of MOPC in the outer membrane monolayer calculated from Eq. AIII.4. The constants of the functional rates that correspond to the constant "off" and "on" rates are the same as their respective counterparts in Fig. 5. Curve 1 is for constant "on" and "off" rates. The coefficients k_{mb1}, k'_{bm1}, and k''_{bm1} are chosen to be of equal magnitude. The coefficients of the "on" rates are chosen to be negative, and the coefficient of the "off" rate is positive. Magnitudes of the coefficients: curve 2, 10^{-14}; curve 3, 10^{-12}; curve 4, 3×10^{-12}; curve 5, 10^{-11}; curve 6, 10^{-10} (the dimensions of these coefficients are the same as the dimensions of their counterparts in Fig. 5). It is seen that the apparent rate of intercalation increases with the increase of the magnitude of the coefficients.

chosen to be of equal magnitude, even though they are of different dimensions (see legend of Fig. 5), because there are no available data for their actual values. It is also assumed that k_{mb1} is positive when the other two coefficients are negative. When the magnitude of the above coefficients is 1×10^{-13} times smaller than k_{mb0} or less, the kinetics is the same as that for a membrane with constant rates. For intermediate values (from 1×10^{-13} to 1×10^{-9} times k_{mb0}), the apparent kinetics is complex, eventually becoming single exponential. When the coefficients are larger than 1×10^{-9} times k_{mb0}, the kinetics is again a single exponential, but the amount of intercalated lysolipid in the membrane is negligible (the exchanged molecule is practically insoluble in the membrane). The desorption kinetics has an apparent rate equal to that of the exchange with constant rates. For the chosen values of the rate coefficients the apparent rate of intercalation is smaller than the apparent rate of desorption.

Eq. 5 predicts that when the rate constants are functions of the amount of intercalated lysolipid, the overall rate of exchange (or the corresponding apparent half-time for the exchange) depends on the concentration of lysolipid in the bathing solution. The dependence of the apparent half-time for exchange on the lysolipid concentration in the bathing solution is shown in Fig. 10. It is seen that the apparent half-time is larger for lower concentrations of MOPC and smaller for higher concentrations of lysolipid.

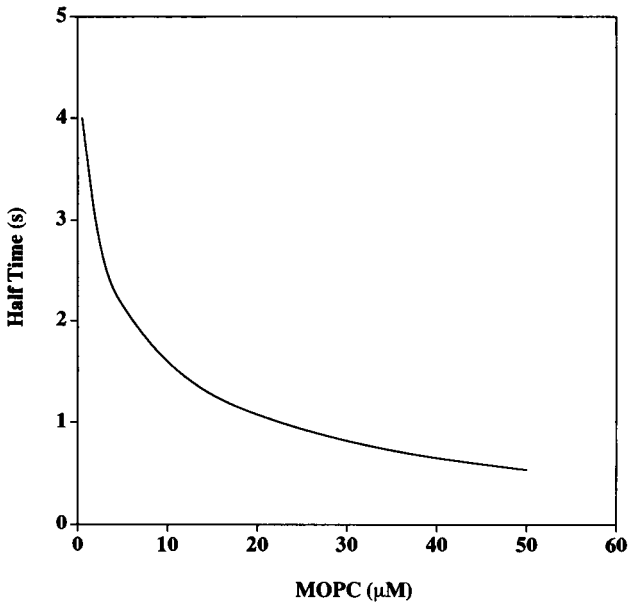

FIGURE 10 Dependence of the half-time of MOPC intercalation on the lysolipid concentration in the bathing solution. (The parameters of the model are the same as those of curve 3 in Fig. 9.)

pH-dependent interbilayer exchange of phosphatidylglycerol

Another example in which the transport kinetics may be affected by the number of transported molecules is the pH-dependent transfer of charged lipids (Hope and Cullis, 1987; Hope et al., 1989; Redelmeier et al., 1990; Eastman et al., 1991; Farge and Devaux, 1992). In this case, the average charge per lipid headgroup (e.g., phosphatidylglycerol) in the two membrane monolayers is different because of the different pH of the bathing solutions at both sides of the membrane. This difference in the concentration of neutral lipid between the two monolayers leads to a net flux of lipid molecules toward the monolayer, with lower concentration of the neutral form. As a result, one of the monolayers is depleted of the exchangeable lipid while the other is enriched. For a vesicle membrane, this leads to an apparent compression of one of the monolayers and an apparent extension of the other, which may also be coupled with a shape change (Farge and Devaux, 1992).

pH-induced transfer of phosphatidylglycerol (PG) is a good candidate for lipid exchange with functional rate. In this case, the apparent rate of PG transfer depends on the initial concentration of PG in the membrane (Redelmeier et al., 1990). Furthermore, there is always a significant amount of PG lipid (from 20% to 50%), which remains in the donor monolayer regardless of the difference of the hydrogen concentration of the two bathing solutions. And finally, PG transfer depends on the presence of other types of lipids that are transferable under the same conditions.

PG transfer is modeled as both a transfer with constant rate and a transfer with functional rate, and the two kinetics are compared. The kinetics of PG transfer with a constant rate is

$$[N_{dm}] = \frac{[N_{PGtot}]}{\left(1 + \frac{C_{dH}}{C_{aH}}\right)} - \left(\frac{[N_{PGtot}]}{\left(1 + \frac{C_{dH}}{C_{aH}}\right)} - [N_{idm}]\right)\exp(-k_f^{exp}t), \quad (6)$$

where $[N_{idm}]$ and $[N_{dm}]$ are the initial and current PG concentrations of the donor monolayer, $[N_{PGtot}]$ is the total PG concentration in the membrane, t is time, k_f^{exp} is the experimentally measured apparent rate of PG transfer, and C_{aH} and C_{dH} are constants characterizing the hydrogen concentration in the bathing solutions bounding the acceptor and the donor monolayer, respectively (see Appendix III).

In Eq. 6, $C_{dH} \gg C_{aH}$, because in the experiments of Redelmeier et al. (1990) the hydrogen concentration in the outside solution is several orders of magnitude larger than the same concentration in the inside solution. Therefore, it is expected that at equilibrium, the concentration of PG in the donor monolayer will be negligible compared to its initial concentration. However, the experimental data of Redelmeier et al. (1990) show that the equilibrium concentration of PG in the donor monolayer is significantly larger than the one predicted by Eq. 6 (see Fig. 11). The authors analyze their data by using the equation

$$[N_{dm}] = [N(eq)] - ([N(eq)] - [N_{idm}])\exp(-k_f^{exp}t) \quad (7)$$

where $[N(eq)]$ is called the equilibrium PG concentration and is determined from the experimental data.

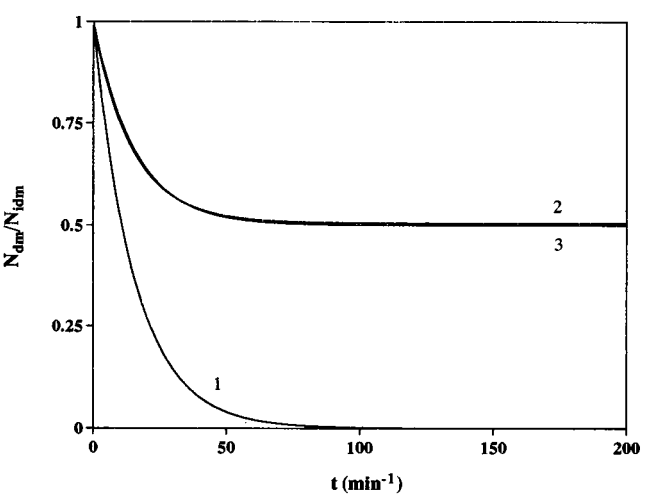

FIGURE 11 Kinetics of pH-induced phosphatidylglycerol (PG) transfer from the donor monolayer of EPC vesicles. Curve 1 is the kinetics of PG transfer with constant rate calculated from Eq. 6; curve 2 is calculated from Eq. 7 and apparently represents the experimentally measured kinetics of PG transfer (Redelmeier et al., 1990); and curve 3 is the kinetics calculated from Eq. AIII.9. Parameters used in the calculations: initial PG concentration $[N_{PGtot}] = 0.1$; $k_c = 10^{-2}$ M (corresponding to the pK_a of PG); $[H_d^+] = 10^{-4}$ M; $[H_a^+] = 10^{-6}$ M; $k_{fp0} = 792\ s^{-1}$; $k_{fp1} = 14850\ s^{-1}$ (all parameters, except for the two rate constants, are from Redelmeier et al., 1990).

The equilibrium PG concentration [N(eq)] depends on the initial PG concentration [N_{PGtot}] and is larger for larger [N_{PGtot}]. A similar dependence of the equilibrium concentration on the MOPC concentration in the bathing solution is predicted by Eq. 5 (see Fig. 9). This similarity of the dependence of the equilibrium concentrations on the initial amount of available lipid suggests that PG transfer may proceed with functional rate. All possible models have been considered (not shown), where the rate of transfer is assumed to be a function of the protonated or the overall amount (including both protonated and charged forms) of PG in one or both of the membrane monolayers. Of these models, the most consistent result is found when the rate of transfer depends on the difference in the overall PG concentrations (including both the protonated and the charged forms) of the two monolayers (see Eq. AIII.8). In this case, the kinetic equation giving the overall rate of PG transfer has the same form as Eq. 5 (see also Eq. AIII.9). The overall kinetics of PG transfer calculated by using Eq. AIII.9 is shown in Fig. 11. It is seen that the two constants k_{fp0} and k_{fp1} allow a good fit to the experimental kinetics (curve 2 in Fig. 11). The apparent half-time of the calculated overall kinetics depends on the magnitude of the above two constants, and the equilibrium PG concentration depends on their ratio.

The values of k_{fp0} and k_{fp1} found from fitting the experimental curve in Fig. 11 are used to calculate the equilibrium PG concentration and the apparent half-time as a function of PG concentration in the membrane. The calculated equilibrium PG concentrations and apparent half-times are shown in Fig. 12, *a* and *b*, respectively. Also shown are the experimentally measured values of the same parameters for 5, 10, 20, and 30 mol% PG. It can be seen that in Fig. 12 *a*, the predicted values of the equilibrium PG concentration are close to the ones measured experimentally. However, the predicted values of the apparent half-time in Fig. 12 *b* are smaller than the ones measured experimentally. One reason for this difference may lie in the fact that, during the experiment, the pH of the internal vesicle solution decreases gradually (Redelmeier et al., 1990). This change in the internal pH, while the outside pH remains constant, is likely to affect the measured apparent half-time. In contrast to the apparent half-time, the equilibrium PG concentration depends mainly on the final values of pH. Therefore, it is less sensitive to the intermediate values of the pH. The agreement of the predicted equilibrium PG concentration and apparent half-time with the experimental data strongly suggests that pH-induced PG transfer proceeds with functional rates.

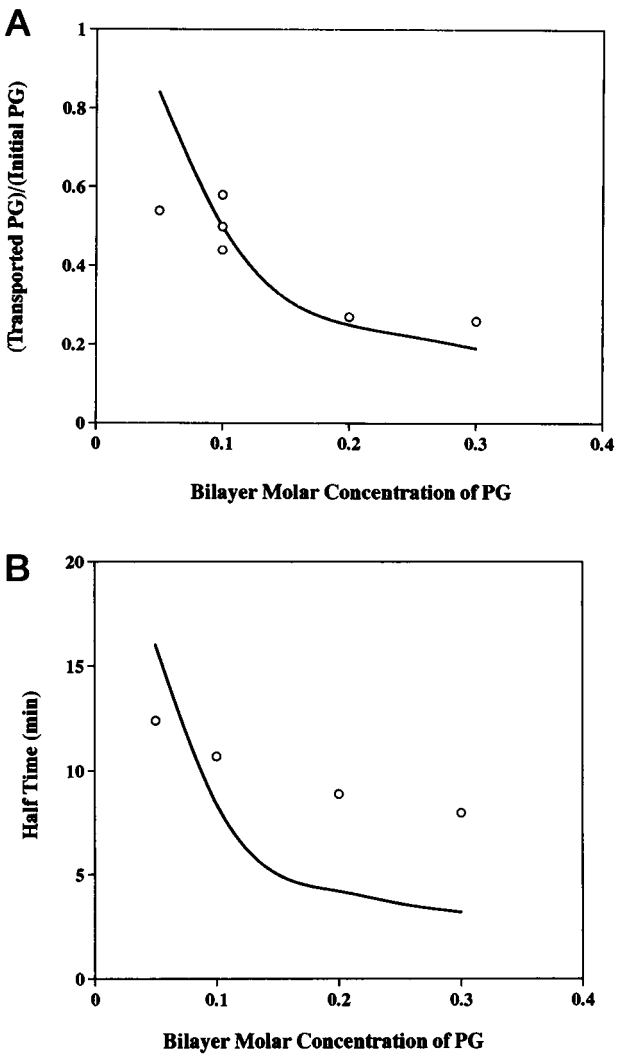

FIGURE 12 Dependence (*a*) of the equilibrium PG concentration in the donor monolayer and (*b*) of the apparent half-time of PG transfer on the concentration of PG in the membrane. The circles show the experimental data from Redelmeier et al. (1990).

DISCUSSION

The passive transport of MOPC includes its exchange between the membrane and the bathing solution, and its transfer between the two membrane monolayers. The overall rate of this transport depends on the rate of desorption ("off" rate) and on the rate of interbilayer transfer. It is important to understand how the above two rates are related to the change in the chemical potential of MOPC molecules when they are transported between their three pools (see Fig. 1). In the following paragraphs is discussed 1) how the measured "off" rate is related to the energy of dissociation of a lysolipid molecule from the membrane; 2) what factors govern the MOPC transport during interbilayer transfer; and 3) how the measured overall kinetics of molecular exchange is used to distinguish between exchange with constant rates and exchange with functional rates.

Rate of lysolipid desorption and energy of dissociation

MOPC exchange depends on its chemical potential in the membrane and in the bathing solution. When these chemical

potentials are different, there is a net flux of lysolipid toward the pool where the chemical potential is lower. Depending on this difference, the exchange proceeds with a certain overall rate. Eqs. 2 and 3 as well as the results shown in Figs. 6 and 8 show that the true "off" rate is found from the experimentally measured apparent rate of fast desorption, when the effect of the stagnant layer is negligible. The fastest measured rate of desorption in the experiments of Needham and Zhelev (1995) is on the order of 0.2 s^{-1}. This apparent rate is taken as an estimate of the true "off" rate and is now used to calculate the activation energy of dissociation of a single hydrocarbon group from the membrane. The activation energy of dissociation per hydrocarbon group is found from the activation energy of dissociation of MOPC divided by the number of its hydrocarbon groups. The activation energy of MOPC dissociation is calculated using the model of Aniansson et al. (1976). According to this model, the "off" rate k_{mb} and the activation energy of dissociation ΔG are related by

$$k_{mb} = \frac{D(\Delta G)^2}{(kTl_{max})^2} \exp\left(-\frac{\Delta G}{kT}\right), \quad (8)$$

where D is the diffusion coefficient of the molecule in the bathing solution, k is the Boltzmann constant, T is the absolute temperature, and l_{max} is the maximum length of the molecular hydrocarbon chain.

In Eq. 8 the diffusion coefficient of a single MOPC monomer in aqueous solution is taken to be on the order of 5×10^{-10} $m^2 \cdot s^{-1}$. The maximum length of the MOPC hydrocarbon chain is calculated from the chain's volume and its minimum cross-sectional area. The volume of the hydrocarbon chain of MOPC is half of the volume of the EPC's double chain. The volume of the hydrocarbon chain of EPC is on the order of 870 $Å^3$, which is the volume of the same quantity for dioleoylphosphatidylcholine (Tardieu et al., 1973). Then the volume of the hydrocarbon chain of MOPC is 435 $Å^3$. The minimum cross-sectional area of a single hydrocarbon chain is on the order of 20 $Å^2$ (Ruocco and Shipley, 1982). Then the value of l_{max} in Eq. 8 is 21.7 Å. Using the experimentally measured rate of desorption and Eq. 8, the calculated activation energy of dissociation is 1.09×10^{-19} J. This value corresponds to 65.5 kJ · mol^{-1} (or 15.7 kcal · mol^{-1}), which gives 0.87 kcal · mol^{-1} per hydrocarbon group. The values for the same activation energy calculated from the exchange of diacyl lipids are smaller. [Examples for these activation energies are 0.68 kcal · mol^{-1} (Israelachvili, 1991); 0.78 kcal · mol^{-1} for the activation energy of phosphatidylcholine lipids (Nichols, 1985); 0.8 kcal · mol^{-1} for dimyristoylphosphatidylethanolamine calculated from the data of Wimley and Thompson (1991); and 0.65 kcal · mol^{-1} for phosphatidylethanolamine lipids (Silvius and Leventis, 1993)]. Elamrani and Blume (1982) measured the kinetics of intercalation of lysopalmitoylphosphatidylcholine in bilayer membranes using a stopped-flow method. The "off" rate determined from their kinetics of lysolipid adsorption is on the order of 0.9 s^{-1}. This corresponds to an activation energy of dissociation per hydrocarbon group on the order of 0.99 kcal · mol^{-1}. It is seen then, that the activation energies calculated for double chain lipids are smaller than their respective counterparts for single-chain lipids. It may be expected that the activation energy for diacyl lipids will be smaller because the two chains are in contact. To calculate the apparent increase of the contact area of a single chain, relative to that of a double chain, it is assumed that the hydrocarbon chain of a dissociating lipid is incompressible and fully extended and makes a single volume. With these assumptions, the circumference of the chain of a dissociating lipid is similar to its circumference in a gel-phase membrane. In the later case, the circumference is calculated by using X-ray data. Abrahamsson et al. (1978) have shown that below phase transition, fully extended lipid chains pack in a hybrid HS2-type lattice. The parameters of this lattice have been measured for dipalmitoylphosphatidylethanolamine and they are a_s = 10 Å, b_s = 7.8 Å, and c_s = 2.5 Å (Abrahamsson et al., 1978). These lattice parameters are similar to the lattice parameters of phosphatidylcholine membranes, because the two lipids have similar packing (Hauser et al., 1981). From the above lattice parameters, the calculated circumference of a single chain is 18.36 Å, and that of a double chain is 27.54 Å. The comparison of the two circumferences shows that the ratio of the circumference of a single chain to half of the circumference of a double chain is 1.33. When the value of the activation energy per hydrocarbon group found for single-chain lipids is divided by the above factor, the corrected activation energy is 0.65 kcal · mol^{-1}. This now is in very good agreement with the same value measured for double-chain lipids. These calculations show that even though the rate of flow in the experiments of Needham and Zhelev (1995) is slower than that in the experiments of Elamrani and Blume (1982), the micropipette method gives a reliable estimate of the true "off" rate of MOPC.

Mechanism of interbilayer transfer

The transport of molecules between the two membrane monolayers is characterized by the rate of interbilayer transfer. This rate is related to the activation energy of transfer of a lipid molecule from one of the monolayers into the other. The transported molecule may cross the membrane separately or may follow a collective motion (molecular flow). In the first case the transport is called "flip-flop," and in the second case it occurs through some kind of membrane defects. It is known that the activation energy of flip-flop depends mainly on the energy barrier for transfer of the lipid headgroup, but also has a minor dependence on the length of the lipid chain (Homan and Pownall, 1988). However, the exact mechanism of this transfer is not known; it is also unknown how its activation energy depends on the thickness of the membrane's hydrophobic region and/or the ratio of the apparent area of the headgroup to the apparent area of

the hydrocarbon chain of the transferred lipid. Molecular transport through membrane defects has not been thoroughly studied. It is expected, that in this case, the activation energy of molecular transfer will depend strongly on the energy of defect formation, and its dependence on physical characteristics of molecular flow will be negligible because of the low viscosity of the membrane.

Because the exact mechanism of flip-flop is not known, the rate k_f is related to the thermodynamic characteristics of the lipid transfer by using a more general version of the activation complex theory than the one used for the interpretation of the "off" rate in the previous section. The generalization of Eq. 8 used in this section is (Glasstone et al., 1941)

$$k_f = \chi \frac{kT}{\hbar}\left(\frac{Z^*}{Z_m}\right)\exp\left(-\frac{E_b}{RT}\right), \tag{9}$$

where χ is the transmission coefficient (usually chosen equal to one); $\hbar$ is Planck's constant; Z^* and Z_m are the partition functions of the activated state and the metastable state, respectively; R is the gas constant; T is the absolute temperature; and E_b is the barrier energy.

Equation 9 has limited use in chemistry because for solutions, the partition coefficient of the activated state is not known. In this case Eq. 9 is commonly replaced by (Glasstone et al., 1941)

$$k_f = \frac{kT}{\hbar}\exp\left(-\frac{\Delta G^{\ddagger}}{RT}\right), \tag{10}$$

where $\Delta G^{\ddagger}$ is the Gibbs energy of activation in standard state.

The advantage of using Eq. 10 compared to Eq. 9 is that the Gibbs energy of activation in standard state is an experimentally measurable parameter. For different temperatures the Gibbs energy of activation is calculated from $\Delta G^{\ddagger} = \Delta H^{\ddagger} - T\Delta S^{\ddagger}$, where the enthalpy $\Delta H^{\ddagger}$ and the entropy $\Delta S^{\ddagger}$ of formation of the activated state are independent of temperature. Both the enthalpy $\Delta H^{\ddagger}$ and the entropy $\Delta S^{\ddagger}$ of formation of the activated state during flip-flop of phosphatidylcholine lipids have been measured by Homan and Pownall (1988). Their values are 36 kcal $\cdot$ mol^{-1} and 0.03 kcal $\cdot$ mol^{-1} $\cdot$ K^{-1}, respectively.

The above values of the enthalpy and entropy of formation of the activated state are used to calculate from Eq. 10 the rate of lipid flip-flop, at the temperature used in the experiments of Needham and Zhelev (1995). This temperature is 14°C, which has a corresponding rate of lipid flip-flop equal to 8×10^{-9} s^{-1}. This value is much smaller than the value on the order of 2×10^{-3} s^{-1}, measured for the rate of lipid transfer in the experiments of Needham and Zhelev (1995). Therefore, it is very unlikely that the lipid transfer in the experiments of Needham and Zhelev (1995) is the result of a molecular flip-flop.

The experimental conditions of Homan and Pownall (1988) for measuring lipid flip-flop are different from the conditions used in the experiments of Needham and Zhelev (1995). In the first case the area per molecule in the two membrane monolayers is the same, whereas in the second case it is not. The difference of the area per molecule in the latter case may affect the rate of interbilayer transfer either by lowering the Gibbs energy of activation or by promoting the formation of short-lived membrane defects. So far, there are no data showing how the thermodynamic parameters of the formation of the activated state ($\Delta G^{\ddagger}$, $\Delta H^{\ddagger}$, and $\Delta S^{\ddagger}$) are to be related to the change of the area per molecule. In contrast to the thermodynamic characteristics, the dependence of defect formation and membrane failure on the area per molecule has been studied more thoroughly (Needham and Nunn, 1990). Furthermore, recent developments of the micropipette method (Zhelev and Needham, 1993) have provided additional information about the lifetime of existing membrane defects (in this case, actual pores). Membrane defects form when both the area per molecule and the corresponding membrane tension reach a certain limit. This limit for the membrane tension is called critical membrane tension. The critical membrane tension for the EPC membrane is 9.6 mN $\cdot$ m^{-1} (McIntosh et al., 1995). This corresponds to a critical tension of one of the monolayers of approximately 5 mN $\cdot$ m^{-1}. As shown earlier, tensions on this order of magnitude are produced when MOPC partitions differently in the membrane monolayers. Indeed, at the end of the fast exchange, the total amount of MOPC in the membrane is 10 to 15 mol%. Because the lysolipid partitions mostly in one of the monolayers, its concentration in this monolayer is 20 to 30 mol%. The result of this partitioning is that a negative tension (or "compression tension") is generated in this monolayer because of molecular crowding. As has already been discussed in the previous sections, the tensions of the two monolayers are coupled. Thus, the generation of the compression tension induces an "extension tension" in the other monolayer. The accumulation of 20 to 30 mol% MOPC in one of the monolayers leads to the generation of a compression tension of 6 mN $\cdot$ m^{-1} and an extension tension of 7 mN $\cdot$ m^{-1}. (The difference of 1 mN $\cdot$ m^{-1} between the two tensions is a result of the applied tension of 1 mN $\cdot$ m^{-1} by the suction pipette.) It can be seen that because of the different partitioning of MOPC in the membrane monolayers, one of them is extended with a tension that is on the order of the critical monolayer tension. This calculation indicates that the fast exchange of lysolipid with one of the monolayers can, in fact, promote the formation of monolayer defects. The lifetime of these defects is expected to be very small (on the order of milliseconds or less; Zhelev and Needham, 1993) compared to the minimum time required to detect any small area change (usually on the order of seconds). This makes it impossible for the membrane defects to be detected by simply observing the measured kinetics of lysolipid uptake or desorption. Taken together, these results suggest that collective lipid transport through short-lived monolayer defects may contribute to the measured apparent rate of lipid transfer in the experiments of Needham and Zhelev (1995).

Exchange with constant rates and exchange with functional rates

For some lipids the rate of exchange depends on the membrane composition (Wimley and Thompson, 1990, 1991). The exchange of MOPC itself results in a change of the composition of the membrane. Therefore, it is expected that the overall rate of exchange will depend on the number of transported molecules. To take this effect into account, the experimental results of Needham and Zhelev (1995) for fast lysolipid exchange are analyzed by using two models: one for the exchange with constant rates and another for the exchange with functional rates. According to these models, the overall rate of exchange is apparently a single exponential (see Figs. 5 and 9). This result shows that the shape of the experimentally measured kinetics cannot be used to distinguish between the two cases. The major difference between the exchange with constant rates and the exchange with functional rates is that in the first case, the apparent half-time is independent of the MOPC concentration in the bathing solution, whereas in the second case it depends on this concentration (Fig. 10). The experimentally measured half-time of MOPC exchange is independent of the lysolipid concentration in the bathing solution; therefore, the exchange of MOPC proceeds with constant rates. In contrast to the exchange of MOPC, the half-time of pH-induced transfer of PG depends on its concentration in the membrane (Redelmeier et al., 1990). Furthermore, the predicted equilibrium PG concentration in the donor monolayer is in good agreement with the experimentally measured values of the same quantity (see Fig. 12). Therefore, the pH-induced transfer of PG is considered to proceed with a functional rate.

CONCLUSION

In conclusion, the kinetics of MOPC exchange with EPC is modeled as a two-step process: the first step is the adsorption-intercalation of the lysolipid in the outer membrane monolayer and the second step is its transfer into the inner monolayer. The first step is faster than the second one. The apparent rate of the first step is largely set by lysolipid desorption via the "off" rate. A reliable estimate of this rate is found by measuring the kinetics of fast MOPC desorption from a vesicle membrane. For the experiments of Needham and Zhelev (1995), this rate is on the order of 0.2 s^{-1}. The "off" rate allows the calculation of the energy of dissociation per hydrocarbon group. This energy for MOPC is 0.87 kcal · mol^{-1}. This value is in good agreement with the same quantity measured for single-chain lipids and for diacyl lipids.

The apparent rate of the second step of lysolipid exchange is limited by the rate of interbilayer transfer. The measured rate of interbilayer transfer of MOPC is on the order of 0.002 s^{-1} (Needham and Zhelev, 1995). This rate is 10^3 times faster that the rate of flip-flop—on the order of 2×10^{-6} s^{-1} (Homan and Pownal, 1988). The difference between the two rates corresponds to a difference of the Gibbs energy of activation on the order of 7 kcal · mol^{-1}. This result shows that the amount of lipid transferred by flip-flop does not account for a substantial part of the transferred lipid during MOPC exchange. The comparison of the generated tension during MOPC exchange with the critical monolayer tension suggests that lipid transport through short-lived membrane defects may contribute to the measured apparent rate of lipid transfer.

APPENDIX I: DEPENDENCE OF THE RELATIVE AREA INCREASE ON THE DISTRIBUTION OF MOPC

It is assumed that the sum of the tension of the inner monolayer τ_i and that of the outer monolayer τ_o is equal to the applied membrane tension τ_α,

$$\tau_\alpha = \tau_i + \tau_o. \tag{AI.1}$$

In the mean field approximation used here, the tension at the effective boundary of a given molecule is equal to the far field tension experienced by the monolayer. When the two monolayers are made of EPC and MOPC, the tensions along the effective boundary of the molecules of every molecular type, in the inner and the outer monolayer, are

$$\tau_i = \frac{K^b}{2}\alpha_i^{e,b} = \frac{K^l}{2}\alpha_i^{e,l}$$
$$\tau_o = \frac{K^b}{2}\alpha_o^{e,b} = \frac{K^l}{2}\alpha_o^{e,l}, \tag{AI.2}$$

where K^b and K^l are the area expansion moduli of the diacyl lipid and lysolipid, respectively, and $\alpha_i^{e,b}$ and $\alpha_o^{e,b}$, and $\alpha_i^{e,l}$ and $\alpha_o^{e,l}$ are the average fractional area changes of the two lipids in the inner and the outer monolayers, respectively.

The initial areas of the inner ($A_{o,in}$) and the outer ($A_{o,out}$) monolayers are equal,

$$A_{o,in} = a_{in}^{b,o}N_{mi}^{b,o}$$
$$A_{o,out} = a_{out}^{b,o}N_{mo}^{b,o}, \tag{AI.3}$$

where $a_{in}^{b,o}$ and $a_{out}^{b,o}$ are the average fractional areas of the bilayer lipid in the inside and outside monolayer, respectively, when the monolayerm tension is equal to $\tau_\alpha/2$, and $N_{mi}^{b,o}$ and $N_{mo}^{b,o}$ are the numbers of molecules in the two monolayers, respectively.

Similarly, during the adsorption-intercalation of MOPC, the areas of the inner (A_{in}) and the outer (A_{out}) monolayers are

$$A_{in} = a_{in}^{b}N_{mi}^{b} + a_{in}^{l}N_{mi}^{l}$$
$$A_{out} = a_{out}^{b}N_{mo}^{b} + a_{out}^{l}N_{mo}^{l}, \tag{AI.4}$$

where a_{in}^{b} and a_{in}^{l}, and a_{out}^{b} and a_{out}^{l} are the average fractional areas of the bilayer lipid and of the lysolipid for monolayer tensions of the inner and outer monolayers equal to τ_i and τ_o, respectively; and N_{mi}^{b} and N_{mi}^{l}, and N_{mo}^{b} and N_{mo}^{l} are the corresponding numbers of molecules of the two molecular types in the two membrane monolayers.

During intercalation the distribution of the transported molecules between the two monolayers may be different. Therefore, the tensions of the monolayers may change, whereas their sum remains constant and equal to the tension imposed by the pipette. The areas of the two monolayers remain equal to each other at all times.

With the above assumptions, the experimentally measured relative area change ($\Delta A/A$) of the vesicle is related to the number of molecules partitioning in the two monolayers by

$$\frac{\Delta A}{A} = \frac{a_o^l}{2A}\left(1 + \frac{\tau_\alpha}{2K^l}\right)(N_{mi}^l + N_{mo}^l) - \frac{\frac{\tau_\alpha}{2}\left(\frac{\Delta A^b}{K^b} + \frac{\Delta A^l}{K^l}\right)^2 + \left(\frac{\Delta A^b}{K^b} + \frac{\Delta A^l}{K^l}\right)(\Delta A^b + \Delta A^l)}{\frac{2Aa_o^b}{K^b}(N_{mi}^b + N_{mo}^b) + \frac{2Aa_o^l}{K^l}(N_{mi}^l + N_{mo}^l)}, \quad \text{(AI.5)}$$

where $\Delta A^b = a_o^b(N_{mi}^b - N_{mo}^b)$ and $\Delta A^l = a_o^l(N_{mi}^l - N_{mo}^l)$ are the differences of the areas occupied by the bilayer lipid and by the lysolipid in the inner and outer monolayers, respectively.

APPENDIX II: LIPID TRANSPORT WITH CONSTANT RATES

Molecular exchange with a single monolayer

During the molecular exchange between a given monolayer and its bathing solution there are two molecular fluxes: one toward the membrane surface J_{bm}, and another toward the bathing solution J_{mo}. These fluxes are proportional to the concentration of the transported molecule in their respective volumes,

$$J_{bm} = k'_{bm}C_{bm}$$
$$J_{mo} = k_{mb}C_{mo}, \quad \text{(AII.1)}$$

where C_{bm} and C_{mo} are the instantaneous concentrations of exchanged molecule in the bathing solution and in the monolayer, respectively (the bulk concentration is defined as the number of molecules per unit volume, whereas the monolayer concentration is the number of molecules per unit area), and k'_{bm} and k_{mb} are the corresponding rate constants. The resultant rate of molecular exchange (dN_{mo}/dt) is found by multiplying the difference of the two fluxes by the contact area A_m between the monolayer and the bathing solution:

$$\frac{dN_{mo}}{dt} = A_m(J_{bm} - J_{mo}) = A_m k'_{bm}C_{bm} - k_{mb}N_{mo}. \quad \text{(AII.2)}$$

In Eq. AII.2 the concentration in the monolayer is expressed through the ratio of the instantaneous number of molecules N_{mo} and the membrane area ($C_{mo} = N_{mo}/A_m$).

Eq. AII.2 can be integrated in time, which gives the instantaneous number of transported molecules. To find the number of transported molecules it is necessary to know their concentration in the adjacent region to the monolayer "interface" in the bathing solution C_{bm}. This concentration depends on the rate of transport in the bathing solution and on the rate of exchange at the "interface." For fast rate of exchange, the solution close to the "interface" may be depleted of the exchanging molecules, which will result in a decrease in the apparent rate of exchange. It is also possible for the exchangeable molecule to be present in the bathing solution in both monomer and micelle form. The above two conditions lead to a different overall kinetics for molecular exchange.

For a fast rate of exchange, the overall kinetics depends on the rate of transport in the bathing solution. To increase the rate of transport in the bathing solution, Needham and Zhelev (1995) placed the vesicle in a flow of solution delivered with a second pipet. Under these conditions the rate of delivery of MOPC to the membrane "interface" is limited by the rate of its transport across the stagnant layer around the vesicle membrane. The shape of the vesicle in these experiments is spherical. It is also assumed that the number of molecules accumulated in the stagnant layer is negligible compared to their number in the membrane. Then, the rate of transport across the stagnant layer is semistationary and the molecular flux across it (dN_c/dt) is proportional to the concentration difference between the membrane "interface" and the region far from the membrane surface (Friedlander, 1957):

$$\frac{dN_c}{dt} = p'(C_{b\infty} - C_{bm}), \quad \text{(AII.3)}$$

where $C_{b\infty}$ is the concentration of the transported molecule far from the membrane "interface," C_{bm} is its concentration at the membrane "interface," and p' is the mass transfer coefficient of the stagnant layer. For a laminar flow around a sphere, the mass transfer coefficient is $p' = R_{out}^2U(3\pi D/8R_{out}U)^{2/3}$ (Friedlander, 1957), where R_{out} is the outside vesicle radius, U is the flow velocity, and D is the diffusion coefficient of the transported molecule in the bathing solution.

The rate of molecular transport across the stagnant layer found from Eq. AII.3 is equal to the rate of molecular exchange with the membrane as defined by Eq. AII.2. Eliminating C_{bm} from Eqs. AII.2 and AII.3 and solving for N_{mo} gives the instantaneous number of intercalated molecules in the monolayer,

$$N_{mo} = \frac{A_m k'_{bm}C_{b\infty}}{k_{mb}} + \left(N_{imo} - \frac{A_m k'_{bm}C_{b\infty}}{k_{mb}}\right)\exp\left(-\left(\frac{k_{mb}}{1 + \frac{A_m k'_{bm}}{p'}}\right)t\right). \quad \text{(AII.4)}$$

When the apparent mass transfer coefficient p^1 of the stagnant layer tends to infinity, the rate constant of Eq. AII.4 is equal to the true "off" rate.

Eq. AII.4 gives the overall kinetics of the exchange of lysolipid monomers with the outside vesicle monolayer. It gives both the kinetics of MOPC intercalation and desorption, when the monomer concentration in the bathing solution is smaller than the CMC. However, the uptake of MOPC occurs both below the CMC and above it. In the later case, the intercalation of MOPC includes both monomer association and micelle fusion. The kinetic equation for this case is derived below.

For adsorption-intercalation above the CMC, the mass transfer coefficient in Eq. AII.3 as well as the "on" rate in Eq. AII.2 are expected to have different values for monomers and for micelles. It is assumed that the monomer concentration in the bathing solution is constant everywhere (including the membrane-water "interface") and is equal to the CMC. In this case, the rate of molecular transport across the stagnant layer (dN_c/dt) has only one component,

$$\frac{dN_c}{dt} = p''(C''_{b\infty} - C''_{bm}), \quad \text{(AII.5)}$$

where $C''_{b\infty}$ is the micelle bulk concentration, C''_{bm} is the micelle concentration at the membrane "interface," and p'' is the mass transfer coefficient of micelles.

Under these conditions the flux of MOPC across the membrane-stagnant layer "interface" has two components—one for monomer intercalation and another for micelle fusion, whereas the flux toward the stagnant layer has only one component—the monomer dissociation. The resultant rate of exchange is

$$\frac{dN_{mo}}{dt} = A_m k'_{bm}\mathrm{CMC} + A_m k''_{bm}C''_{bm} - k_{mb}N_{mo}, \quad \text{(AII.6)}$$

where the quantities have the same meaning as their respective counterparts in Eqs. AII.1 and AII.2. (The single primes in Eq. AII.6 stand for quantities related to monomers, and double primes for quantities related to micelles.)

The overall kinetics of lysolipid adsorption-intercalation above the CMC is

$$N_{mo} = \frac{A_m(k'_{bm}CMC + k''_{bm}C''_{b\infty}}{k_{mb}} + \left(N_{imo} - \frac{A_m(k'_{bm}CMC + k''_{bm}C''_{b\infty}}{k_{mb}}\exp\left(-\left(\frac{k_{mb}}{1 + \frac{A_m k''_{bm}}{p''}}\right)t\right)\right). \quad \text{(AII.7)}$$

Molecular exchange with the whole bilayer membrane

For long time intervals, the exchange of MOPC with the whole bilayer membrane includes both intercalation into the outer monolayer and transfer into the inner monolayer. In the experiments of Needham and Zhelev (1995), the amount of MOPC in the vesicle interior is negligible compared to its amount in the membrane; therefore, the exchange with the vesicle interior is neglected. As in the case of exchange with a monolayer, the concentration of lysolipid in the bathing solution can be above or below the CMC. Similarly, two cases are considered: adsorption-intercalation and desorption below the CMC; and adsorption-intercalation above the CMC. In the first case the rate of molecular transport across the stagnant layer is given by Eq. AII.3. The rate of exchange with the outer monolayer (dN_{mo}/dt) is now

$$\frac{dN_{mo}}{dt} = A_m k'_{bm} C'_{bm} - k_{mb} N_{mo} - k_f N_{mo} + k_f N_{mi}, \quad \text{(AII.8)}$$

where k_f is the rate of interbilayer transfer and N_{mi} is the number of MOPC molecules in the inner monolayer.

The rate of transfer into the inner monolayer (dN_{mi}/dt) *is*

$$\frac{dN_{mi}}{dt} = k_f N_{mo} - k_f N_{mi}. \quad \text{(AII.9)}$$

The solution of the set of equations AII.3 or AII.5, AII.8, and AII.9 gives the overall kinetics of molecular exchange with a bilayer membrane:

$$N_m = \sum_{i=0}^{2}\prod_{j\neq i}^{j=0,2}\frac{\exp(s_i t)}{(s_i - s_j)}\left(s_i(s_i + 2k_f)N_{imo} + s_i\left(s_i + \frac{k_{mb}}{\beta} + 2k_f\right)\right. \quad \text{(AII.10)}$$
$$\left. \cdot N_{imi} + (s_i + 2k_f)\eta\right),$$

where N_{imo} and N_{imi} are the initial concentrations of MOPC in the inner and the outer monolayers, respectively, below the CMC ($\beta = 1 + A_m k'_{bm}/p'$) and ($\eta = A_m k'_{bm} C'_{b\infty}/\beta$), and the coefficients s_i ($i = 0, 1, 2$) are

$$s_0 = 0,$$

$$s_{1,2} = -\frac{1}{2}\left[\left(2k_f + \frac{k_{mb}}{\beta}\right) \pm \left(4k_f^2 + \left(\frac{k_{mb}}{\beta}\right)^2\right)^{\frac{1}{2}}\right].$$

Eq. AII.10 also gives the kinetics of adsorption-intercalation above the CMC when

$$\beta = 1 + \frac{A_m k''_{bm}}{p''}$$

and

$$\eta = \frac{A_m(k'_{bm}CMC + k''_{bm}C''_{b\infty}}{\beta}.$$

APPENDIX III: LIPID TRANSPORT WITH FUNCTIONAL RATES

Exchange with a monolayer

The rate of MOPC exchange with the outer monolayer of the vesicle is

$$\frac{dN_{mo}}{dt} = A_m k'_{bm} C'_{bm} + A_m k''_{bm} C''_{bm} - k_{mb} N_{mo}, \quad \text{(AIII.1)}$$

where C'_{bm} and C''_{bm} are the monomer and micelle concentrations in the bathing solution, respectively. (The monomer concentration is either less than or equal to the CMC. When it is less than the CMC the micelle concentration C''_{bm} is zero.) The "on" and the "off" rates in Eq. AIII.1 are

$$\begin{aligned} k'_{bm} &= k'_{bm0} + k'_{bm1} N_{mo} \\ k''_{bm} &= k''_{bm0} + k''_{bm1} N_{mo} \\ k_{mb} &= k_{mb0} + k_{mb1} N_{mo}, \end{aligned} \quad \text{(AIII.2)}$$

where k'_{bm0}, k''_{bm0}, k_{mb0}, k'_{bm1}, k''_{bm1}, and k_{mb1} are constants.

After substituting the "on" and "off" rates in Eq. AIII.1, the rate of molecular exchange becomes

$$\frac{dN_{mo}}{dt} = -k_{mb1}N_{mo}^2 - (k_{mb0} - A_m(k'_{bm1}C'_{bm} + k''_{bm1}C''_{bm})) \cdot N_{mo} + A_m(k'_{bm0}C'_{bm} + k''_{bm0}C''_{bm}). \quad \text{(AIII.3)}$$

This is a Riccati equation, and its solution is

$$N_{mo} = f_0 - f_1\frac{\exp(-t\sqrt{b^2 + 4ac})}{f_2 + \exp(-t\sqrt{b^2 + 4ac})}, \quad \text{(AIII.4)}$$

where

$$f_0 = \frac{-b + \sqrt{b^2 + 4ac}}{2a}$$

$$f_1 = \frac{\sqrt{b^2 + 4ac}}{a}$$

$$f_2 = \frac{2aN_{imo} + b + \sqrt{b^2+4ac}}{-b - 2aN_{imo} + \sqrt{b^2 + 4ac}},$$

and

$$a = k_{mb1}$$

$$b = k_{mb0} - A_m(k'_{bm1}C'_{bm} + k''_{bm1}C''_{bm})$$

$$c = A_m(k'_{bm0}C'_{bm} + k''_{bm0}C''_{bm}).$$

pH-induced interbilayer transfer

pH-induced PG transfer leads to a difference in the partitioning of the transferable lipid between the two membrane monolayers. The partitioning in one of the monolayers increases (acceptor monolayer), whereas in the

other it decreases (donor monolayer). During the transfer, only the protonated form of the lipid is transported (Redelmeier et al., 1990). The amount of transported protonated lipid depends on its concentration in the two monolayers. For a given monolayer, this concentration is assumed to be proportional to the hydrogen concentration of the bathing solution next to this monolayer and to the PG monolayer concentration (including both the protonated and the charged forms). This assumption is equivalent to the assumption that the rate of PG protonation is much faster than the rate of PG transfer, and therefore, the protonated and charged forms are always close to equilibrium. With this assumption, the concentration of protonated PG in a given monolayer is

$$[N_{dmp}] = \frac{[H_d^+]}{(k_c + [H_d^+])}[N_{dm}] = C_{dH}[N_{dm}]$$

$$[N_{amp}] = \frac{[H_a^+]}{(k_c + [H_a^+])}[N_{am}] = C_{aH}[N_{am}] \quad \text{(AIII.5)}$$

where $[N_{dmp}]$ and $[N_{amp}]$ are the concentrations of protonated PG in donor and acceptor monolayer, respectively; k_c is the hydrogen-PG dissociation constant; $[H_d^+]$ and $[H_a^+]$ are the hydrogen concentrations of the bathing solutions next to the donor and the acceptor monolayer, respectively; and $[N_{dm}]$ and $[N_{am}]$ are the PG concentrations (including both the protonated and the charged forms) of the donor and the acceptor monolayer, respectively. (Note: The concentration of PG in its different forms in the two membrane monolayers is defined as the mole ratio $[N_{PG}] = N_{PG}/N_{all}$, where $[N_{PG}]$ stands for the concentration of any given PG species, N_{PG} is the number of molecules of this species in a given lipid pool, and N_{all} is the number of all molecules partitioning in the membrane.)

The total number of PG molecules N_{PGtot} as well as the number of all molecules N_{all} partitioning in the membrane are preserved. Thus, the sum of PG concentrations in the two membrane monolayers is constant and is equal to the total membrane PG concentration $[N_{PGtot}]$,

$$[N_{dm}] + [N_{am}] = [N_{PGtot}] = \text{constant.} \quad \text{(AIII.6)}$$

With the above assumptions the rate of transfer of protonated lipid from the donor monolayer is

$$\frac{d[N_{dmp}]}{dt} = -(k_{fp}^{da}C_{dH} + k_{fp}^{ad}C_{aH})[N_{dmp}] + k_{fp}^{ad}C_{aH}[N_{PGtot}], \quad \text{(AIII.7)}$$

where k_{fp}^{da} and k_{fp}^{ad} are rate "constants" of transfer of protonated PG from the donor monolayer to the acceptor monolayer and vice versa.

The rate "constants" are assumed to be functions of the difference of PG concentration of the two monolayers,

$$k_{fp}^{ad} = f_{fp0} - k_{fp1}([N_{am}] - [N_{dm}])$$

$$k_{fp}^{da} = k_{fp0} - k_{fp1}([N_{dm}] - [N_{am}]), \quad \text{(AIII.8)}$$

where k_{fp0} and k_{fp1} are constants.

When $k_{fp1} = 0$, Eq. AIII.7 is identical to the equation used by Redelmeier et al. (1990) to model pH-induced PG transfer. The solution of this equation is Eq. 6. It is seen that in the case of PG transfer with constant rate, it is very difficult to introduce, in a consistent manner, the equilibrium PG concentration as it appears in Eq. 7. When $k_{fp1} \neq 0$, the solution of Eq. AIII.7 is given by an equation similar to Eq. AIII.4,

$$[N_{dm}] = \frac{f_0}{C_{dH}} - \frac{f_1}{C_{dH}} \frac{\exp(-t\sqrt{b^2 + 4ac})}{(f_2 + \exp(-t\sqrt{b^2 + 4ac}))}, \quad \text{(AIII.9)}$$

where

$$f_0 = \frac{-b + \sqrt{b^2 + 4ac}}{2a}$$

$$f_1 = \frac{\sqrt{b^2 + 4ac}}{a}$$

$$f_2 = \frac{2a[N_{idmp}] + b + \sqrt{b^2 + 4ac}}{-b - 2a[N_{idmp}] + \sqrt{b^2 + 4ac}},$$

where $[N_{idmp}]$ is the initial concentration of protonated PG in the donor monolayer and

$$a = 2k_{fp1}\left(1 - \frac{C_{aH}}{C_{dH}}\right)$$

$$b = k_{fp0}(C_{aH} + C_{dH}) + k_{fp1}[N_{PGtot}](3C_{aH} - C_{dH})$$

$$c = (k_{fp0} + k_{fp1}[N_{PGtot}])C_{aH}C_{dH}[N_{PGtot}].$$

The author is grateful to Drs. D. Needham, S. Simon, and R. M. Hochmuth of Duke University and to Dr. A. Parsegian of the National Institutes of Health for the helpful discussions.

This work is supported by grants 2 RO1 HL23728 and GM 40162 from the National Institutes of Health and a grant from the Whitaker Foundation.

REFERENCES

Abrahamsson, S., B. Dahlen, H. Lofgren, and I. Pascher. 1978. Lateral packing of hydrocarbon chains. *Prog. Chem. Fats Other Lipids.* 16: 125–143.

Aniansson, E. A. G., S. N. Wall, M. Almgen, H. Hoffmann, I. Kielmann, W. Ulbricht, R. Zana, J. Lang, and C. Tondre. 1976. Theory of the kinetics of micellar equilibria and quantitative interpretation of chemical relaxation studies of micellar solutions of ionic surfactants. *J. Phys. Chem.* 80:905–922.

Asaoka, Y., K. Yoshida, Y. Sasaki, Y. Nishizuka, M. Murakami, I. Kudo, and K. Inoue. 1993. Possible role of mammalian secretory group II phospholipase A_2 in T-lymphocyte activation: implication in propagation of inflammatory reaction. *Proc. Natl. Acad. Sci. USA.* 90:716–719.

Baker, B. L., B. C. Blaxall, D. A. Reese, G. R. Smith, and J. D. Bell. 1994. Quantification of the interaction between lysolecithin and phospholipase A_2. *Biochim. Biophys. Acta.* 1211:289–300.

Besterman, J. M., and P. L. Domanico. 1992. Association and metabolism of exogenously-derived lysophosphatidylcholine by cultured mammalian cells: kinetics and mechanisms. *Biochemistry.* 31:2046–2056.

Brown, D. S., B. L. Baker, and J. D. Bell. 1993. Quantification of the interaction of lysolecithin with phosphatidylcholine vesicles using bovine serum albumin: relevance to the activation of phospholipase A_2. *Biochim. Biophys. Acta.* 1168:13–22.

Daleke, D. L., and W. H. Huestis. 1985. Incorporation and translocation of aminophospholipids in human erythrocytes. *Biochemistry.* 24: 2406–2416.

Eastman, S. J., M. J. Hope, and P. R. Cullis. 1991. Transbilayer transport of phosphatidic acid in response to transmembrane pH gradients. *Biochemistry.* 30:1740–1745.

Elamrani, K., and A. Blume. 1982. Incorporation kinetics of lysolecithin into lecithin vesicles. Kinetics of lysolecithin-induced vesicle fusion. *Biochemistry.* 21:521–526.

Farge, E., and Devaux, P. D. 1992. Shape changes of giant liposomes induced by an asymmetric transmembrane distribution of phospholipids. *Biophys. J.* 61:347–357.

Ferrell, J. E., K.-J. Lee, and W. H. Huestis. 1985a. Membrane bilayer balance and erythrocyte shape: a quantitative assessment. *Biochemistry.* 24:2849–2857.

Ferrell, J. E., K.-J. Lee, and W. H. Huestis. 1985b. Lipid transfer between phosphatidylcholine vesicles and human erythrocytes: exponential decrease in rate with increasing acyl chain length. *Biochemistry.* 24: 2857–2864.

Fettiplace, R., and D. A. Haydon. 1980. Water permeability of lipid membranes. *Physiol. Rev.* 60:510–550.

Friedlander, S. K. 1957. Mass and heat transfer to single spheres and cylinders at low Reynolds numbers. *American Institute of Chemical Engineers Journal.* 3:43–48.

Glasstone, S., K. J. Laidler, and H. Eyring. 1941. The Theory of Rate Processes. McGraw-Hill Co., New York.

Golan, D. E., C. S. Brown, C. M. L. Cianci, S. T. Furlong, and J. P. Caulfield. 1986. Schistosomula of *Schistosoma mansoni* use lysophosphatidylcholine to lyse adherent human red blood cells and immobilize red cell membrane components. *J. Cell Biol.* 103:819–828.

Hauser, H., I. Pascher, R. H. Pearson, and S. Sundell. 1981. Preferred conformation and molecular packing of phosphatidylethanolamine and phosphatidylcholine. *Biochim. Biophys. Acta.* 650:21–51.

Hoffman, R. D., M. Kligerman, T. M. Sundt, N. D. Anderson, and H. S. Shin. 1982. Stereospecific chemoattraction of lymphoblastic cells by gradients of lysophosphatidylcholine. *Proc. Natl. Acad. Sci. USA.* 79: 3285–3289.

Homan, R., and H. Pownall. 1988. Transbilayer diffusion of phospholipids: dependence on headgroup structure and acyl chain length. *Biochim. Biophys. Acta.* 938:155–166.

Hope, M. J., and P. R. Cullis. 1987. Lipid asymmetry induced by transmembrane pH gradients in large unilamellar vesicles. *J. Biol. Chem.* 262:4360–4366.

Hope, M. J., T. E. Redelmeier, K. F. Wong, W. Rodrigueza, and P. R. Cullis. 1989. Phospholipid asymmetry in large unilamellar vesicles induced by transmembrane pH gradients. *Biochemistry.* 28:4181–4187.

Israelachvili, I. N. 1991. Intermolecular and Surface Forces. Academic Press, San Diego, CA.

Kume, N., M. I. Cybulsky, and M. A. Gimbrone, Jr. 1992. Lysophosphatidylcholine, a component of artherogenic lipoproteins, induces mononuclear leucocyte adhesion molecules in cultured human and rabbit arterial endothelial cells. *J. Clin. Invest.* 90:1138–1144.

Mangin[4], E. L., K. Kugiyama, J. H. Nguy, S. A. Kerns, and P. D. Henry. 1993. Effects of lysolipids and oxidatively modified low density lipoprotein on endothelium-dependent relaxation of rabbit aorta. *Circ. Res.* 72:161–166.

Marsh, D. 1990. CRC Handbook of Lipid Bilayers. CRC Press, Inc., Boca Raton, FL.

McIntosh, T. J., S. Advani, R. E. Burton, D. V. Zhelev, D. Needham, and S. Simon. 1995. Experimental tests for protrusion and undulation pressures in phospholipid bilayers. *Biochemistry.* 34:8520–8532.

McIntosh, T. J., and S. A. Simon. 1986. Hydration force and bilayer deformation: a reevaluation. *Biochemistry.* 25:4058–4066.

Nakano, T., E. W. Raines, J. A. Abraham, M. Klagsburn, and R. Ross. 1994. Lysophosphatidylcholine upregulates the level of heparin-binding epidermal growth factor-like growth factor mRNA in human monocytes. *Proc. Natl. Acad. Sci. USA.* 91:1069–1073.

Naraba, H., Y. Imai, M. Hayashi, and S. Oh-ishi. 1993. Enhanced production of platelet-activating factor in stimulated rat leucocytes caused by the blockade of lysophospholipid acylation. *Jpn. J. Pharmacol.* 61: 109–113.

Needham, D., and R. S. Nunn. 1990. Elastic deformation and failure of lipid membranes containing cholesterol. *Biophys. J.* 58:997–1009.

Needham, D., and D. V. Zhelev. 1995. Lysolipid exchange with lipid vesicle membranes. *Ann. Biomed. Eng.* 23:287–298.

Nichols, J. W. 1985. Thermodynamics and kinetics of phospholipid monomer-vesicle interaction. *Biochemistry.* 24:6390–6398.

Quinn, M. T., S. Parthasarathy, and D. Steinberg. 1988. Lysophosphatidylcholine: a chemotactic factor for human monocytes and its potential role in atherogenesis. *Proc. Natl. Acad. Sci. USA.* 85:2805–2809.

Redelmeier, T. E., M. J. Hoppe, and P. R. Cullis. 1990. On the mechanism of transbilayer transport of phosphatidylglycerol in response to transmembrane pH gradients. *Biochemistry.* 29:3046–3053.

Ruocco, M. J., and G. G. Shipley. 1982. Characterization of the subtransduction of hydrated dipalmitoylphosphatidylcholine bilayers. *Biochim. Biophys. Acta.* 691:309–320.

Saito, T., A. Wolf, N. K. Menon, M. Saeed, and R. J. Bing. 1988. Lysolecithins as endothelium-dependent vascular smooth muscle relaxants that differ from endothelium-derived relaxing factor (nitric oxide). *Proc. Natl. Acad. Sci. USA.* 85:8246–8250.

Shier, W. T., J. H. Baldwin, M. Nilsen-Hamilton, R. T. Hamilton, and N. M. Thanassi. 1976. Regulation of guanylate and adenylate cyclase activities by lysolecithin. *Proc. Natl. Acad. Sci. USA.* 73:1586–1590.

Silvius, J. R., and R. Leventis. 1993. Spontaneous interbilayer transfer of phospholipids: dependence on acyl chain composition. *Biochemistry.* 32:13318–13326.

Storch, J., and A. M. Kleinfeld. 1986. Transfer of long-chain fluorescent free fatty acids between unilamelar vesicles. *Biochemistry.* 25: 1717–1726.

Tardieu, A., V. Luzzati, and F. C. Reman. 1973. Structure and polymorphism of the hydrocarbon chains of lipids: a study of lecithin-water phases. *J. Mol. Biol.* 75:711–733.

Van Echteld, C. J. A., B. De Kruijff, J. G. Mandersloot, and J. De Gier. 1981. Effects of lysophosphatidylcholines on phosphatidylcholine and phosphatidylcholine/cholesterol liposome systems as revealed by ^{31}P-NMR, electron microscopy and permeability studies. *Biochim. Biophys. Acta.* 649:211–220.

Vogel, S. S., E. A. Leikina, and L. V. Chernomordik. 1993. Lysophosphatidylcholine reversibly arrests exocytosis and viral fusion at a stage between triggering and membrane merger. *J. Biol. Chem.* 268: 25764–25768.

Wimley, W. C., and T. E. Thompson. 1990. Exchange and flip-flop of dimyristoylphosphatidylcholine in liquid-crystalline, gel, and two-component, two-phase large unilamellar vesicles. *Biochemistry.* 29: 1296–1303.

Wimley, W. C., and T. E. Thompson. 1991. Transbilayer and interbilayer phospholipid exchange in dimyristoylphosphatidylcholine/dimyristoylphosphatidylethanolamine large unilamellar vesicles. *Biochemistry.* 30:1702–1709.

Zhelev, D. V., and D. Needham. 1993. Tension-stabilized pores in giant vesicles: determination of pore size and pore line tension. *Biochim. Biophys. Acta.* 1147:89–104.